NOTE *Internal Medicine*

Ultrasound, CT and FDG PET-CT of a Duodenal Granuloma in a Dog

Sunghoon JEON[1)#], Seong Young KWON[2)#], Rohani CENA[1)], Ju-hwan LEE[3)], Kyoung-Oh CHO[1)], Jung-Joon MIN[2)] and Jihye CHOI[1)]*

[1)]*College of Veterinary Medicine, Chonnam National University, Gwangju 500–757, South Korea*
[2)]*Department of Nuclear Medicine, Chonnam National University Hwasun Hospital, Jeonnam 519–763, South Korea*
[3)]*Chonnam National University Veterinary Teaching Hospital, Gwangju 500–757, South Korea*

(Received 16 December 2013/Accepted 31 March 2014/Published online in J-STAGE 18 April 2014)

ABSTRACT. A 12-year-old spayed female Yorkshire Terrier with intermittent vomiting was diagnosed with regional granulomatous enteritis through histopathological examination. On ultrasonography and computed tomography, a focal thickened duodenal wall showed a mass-like appearance with indistinct wall layers. Marked uptake of ^{18}F-fluorodeoxyglucose was observed from the mass on positron emission tomography-computed tomography. Regional granulomatous enteritis is a rare form of inflammatory bowel disease and may have imaging features similar to intestinal tumors. This is the first study describing the diagnostic imaging features of ultrasonography, computed tomography and positron emission tomography-computed tomography for regional granulomatous enteritis in a dog.
KEY WORDS: canine, computed tomography, duodenum, granuloma, positron emission tomography.

doi: 10.1292/jvms.13-0627; *J. Vet. Med. Sci.* 76(7): 1073–1077, 2014

In veterinary medicine, the term "inflammatory bowel disease (IBD)" is applied to idiopathic inflammation in the intestinal tissues with no identified underlying causes [8]. Idiopathic IBD is classified into types depending on the predominant cells, such as the lymphocytic-plasmacytic, eosinophilic and granulomatous types, in the small intestine [4, 8]. Among them, regional granulomatous enteritis has been reported in only two dogs [1, 10]. Here, we describe the diagnostic features of ultrasonography, computed tomography (CT) and positron emission tomography-computed tomography (PET-CT) for regional granulomatous enteritis in a dog. To the authors' knowledge, this is the first report on diagnostic imaging of regional granulomatous enteritis in veterinary medicine.

A 12-year-old spayed female Yorkshire Terrier was presented with intermittent vomiting for 5 days. Six months previously, ovariohysterectomy was performed, because of an ovarian granulosa cell tumor. On physical examination, abdominal palpation revealed a firm, tubular mass in the left cranial abdomen. The dog's complete blood count was unremarkable. Serum biochemistry demonstrated mildly increased alanine aminotransferase (184 U/*l*; reference limits, 10–100 U/*l*), alkaline phosphatase (237 U/*l*; reference limits, 23–212 U/*l*), gamma-glutamyl transferase (32 U/*l*; reference limits, 0–7 U/*l*) and globulin (4.6 g/d*l*; reference limits, 2.5–4.5 g/d*l*).

Abdominal radiographs revealed no remarkable findings. Ultrasonography revealed a heterogeneous hypoechoic mass, about 1.5 cm in diameter, caudolateral to the left kidney (Fig. 1A). A blood flow signal was observed within the mass in color Doppler mode. In the right cranial quadrant, the wall of the descending duodenum was eccentrically thickened (12 mm thick) and showed a mass-like appearance with indistinct wall layers. In particular, the muscularis layer looked thicker in this portion of the duodenum compared with the rest of the duodenum (Fig. 1B). The mucosal layer showed a heterogeneous hypoechoic change, and the serosal layer had lost its distinct border. The duodenal lumen was considered to be patent based on the movement of gas and fluid through the lumen and the lack of duodenal dilation proximal to the lesion. There were no signs of perforation, such as free fluid, regional lymphadenopathy and free air.

CT and PET-CT examinations were performed to investigate the characteristics of the left abdominal mass and the duodenal wall thickening, to investigate the relationship between the two lesions and to identify metastasis. A CT examination using a 16-row multi-detector CT scanner (Somatom Emotion, Siemens, Forchheim, Germany) was performed at 150 mAs and 110 kV with a 1 mm slice thickness. A contrast study was performed 3 min after intravenous injection of 880 mgI/kg iohexol (Omnipaque 300, GE Healthcare, Shanghai, P.R. China) at a rate of 3 m*l*/sec with a power injector (Medrad Vistron C-T Injector System, Medrad, Inc., Minneapolis, MN, U.S.A.). The left abdominal mass was hypoattenuating (48.1 ± 7.9 HU) and caudal to the left kidney. It showed heterogeneously strong contrast enhancement (167.8 ± 8.6 HU) and had a distinct border dividing it from the enhanced left kidney (270.6 ± 9.0 HU) (Fig. 2). The abdominal mass was not associated with adjacent organs, and the mass was suspected to have originated from the mesentery. The descending duodenum mass was isoattenuating (45.1 ± 3.6 HU) compared with the adjacent intestinal wall and was approximately 4.2 cm in length and 2.5 cm in height. In the post-contrast CT images, the duo-

*CORRESPONDENCE TO: CHOI, J., College of Veterinary Medicine, Chonnam National University, Yongbong-ro, Buk-gu, Gwangju 500–757, South Korea. e-mail: imsono@chonnam.ac.kr

©2014 The Japanese Society of Veterinary Science

This is an open-access article distributed under the terms of the Creative Commons Attribution Non-Commercial No Derivatives (by-nc-nd) License <http://creativecommons.org/licenses/by-nc-nd/3.0/>.

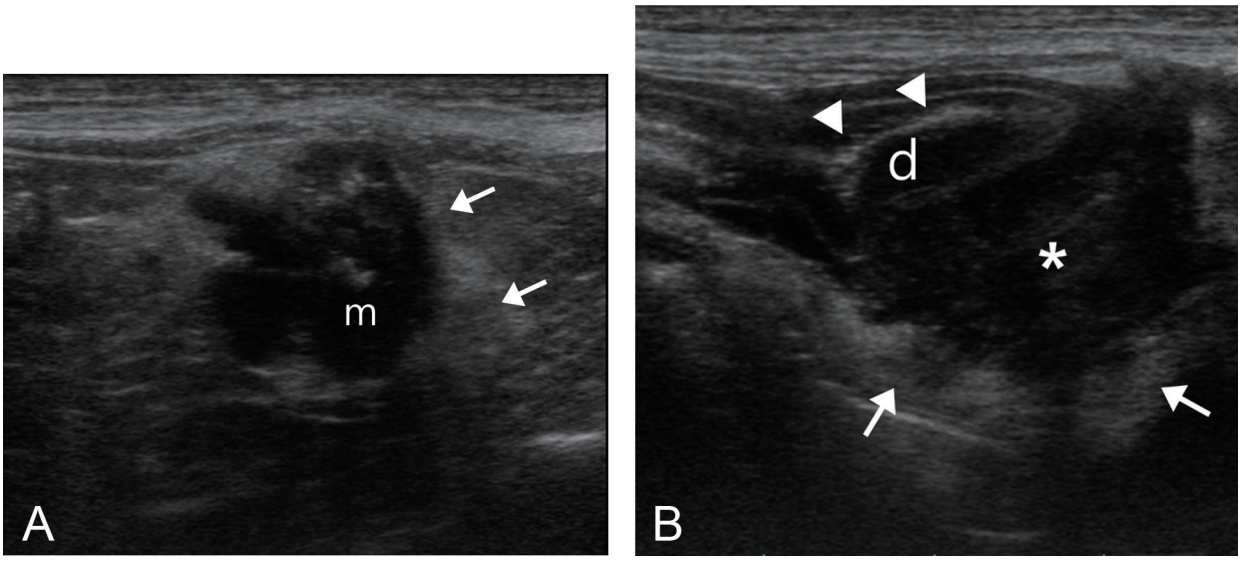


Fig. 1. (A) Ultrasonography of the mass caudal to the left kidney. The hypoechoic mass (m) had ill-defined margins and was surrounded by a hyperechoic mesentery (arrows). (B) Ultrasonography of the duodenal mass (d). The thickened duodenal wall (*) in the far field was seen to involve mucosal and muscular layers compared with the normal wall layers in the near field. The hyperechoic adjacent mesentery (arrows) was consistent with edema or inflammation. The hyperechoic line (arrowheads) is the duodenal lumen with a small volume of gas.

denal mass was markedly enhanced (145.4 ± 14.4 to 161.1 ± 19.2 HU); in particular, the mucosal layer showed higher enhancement compared with the muscular layer. There was no evidence of duodenal obstruction, mottling of mesenteric fat or regional lymphadenopathy. The duodenal mass and left abdominal mass seemed to be connected by a strand of tissue in CT images.

Within three days after the CT examination, PET-CT (Discovery 600 PET/CT system, GE Healthcare, Milwaukee, WI, U.S.A.) was performed at 50 min after intravenous injection of 11 MBq/kg ^{18}F-fluorodeoxyglucose (FDG). The patient was anesthetized before injection of FDG. During PET-CT, non-contrast-enhanced CT (Helical, 8 slice, 120 kVp, 80 mAs, 3.79-mm slice thickness) was performed for attenuation correction, and then, an emission scan was performed with a duration time of 3 min per bed (5 beds in all). Acquired data were reconstructed using ordered subset expectation maximization reconstruction (128 × 128 matrix, 3.27-mm slice thickness, 21 subsets and 2 iterations). There was strong FDG uptake by the duodenal mass as well as by the left abdominal mass (Fig. 3). The maximal standardized uptake values for each mass were 11.0 and 7.3, respectively. There was no metabolic evidence of malignancy in parts of the body other than duodenal and left abdominal masses. The combined imaging studies defined a diagnosis of pathologically active duodenal and mesenteric masses. The differential list for the duodenal mass included primary intestinal neoplasia and, less likely, granulomatous inflammation. The left abdominal mass was suspected to be a granuloma due to the history of recent surgery with neoplasia as a second differential diagnosis.

Because of progressive vomiting, a partial obstruction of the duodenum was suspected, and surgical excision of both masses was planned. At laparotomy, the duodenal mass was found to have arisen from the wall of the descending duodenum and to have expanded by about 3 cm. It was an intramural mass, which ran through the circumference of the wall with a pink to red color and was firm on palpation. The left abdominal mass was located caudal to left kidney and adhered to it. The mass also had a pink to reddish color and an indistinct border with adjacent mesentery tissues. There was no connection between the abdominal mass and duodenal mass, which was contrary to the CT findings. Intestinal resection and anastomosis were performed, and the abdominal mass was removed. After surgery, the dog recovered and was fed a semiliquid diet for 3 days. The dog was rechecked after 1 month and did not exhibit any clinical signs.

The duodenal mass was diagnosed as a sterile pyogranuloma histopathologically (Fig. 4). The infectious organisms were investigated by histopathological examination using special stains including Periodic acid-Schiff, Ziehl-Neelsen acid-fast, Gram and Wright-Giemsa stains and found to be negative. The left abdominal mass was diagnosed as pyogranulomatous and lymphocytic nodular steatitis, and infectious organisms were also ruled out using special stains. Nonabsorbable sutures used in the previous ovariohysterectomy were identified and were suspected as the cause of the steatitis.

Regional granulomatous enteritis, one of the idiopathic IBDs, has been reported in only two dogs [1, 10]. The ileum, jejunum and pylorus were affected in the two dogs. Regional granulomatous enteritis is consistent with Crohn's disease, a major type of IBD, in humans. Crohn's disease is characterized by a transmural granulomatous inflammation of the intestine [11]. This disease mainly affects both the colon and terminal ileum, even though it can affect any portion of the

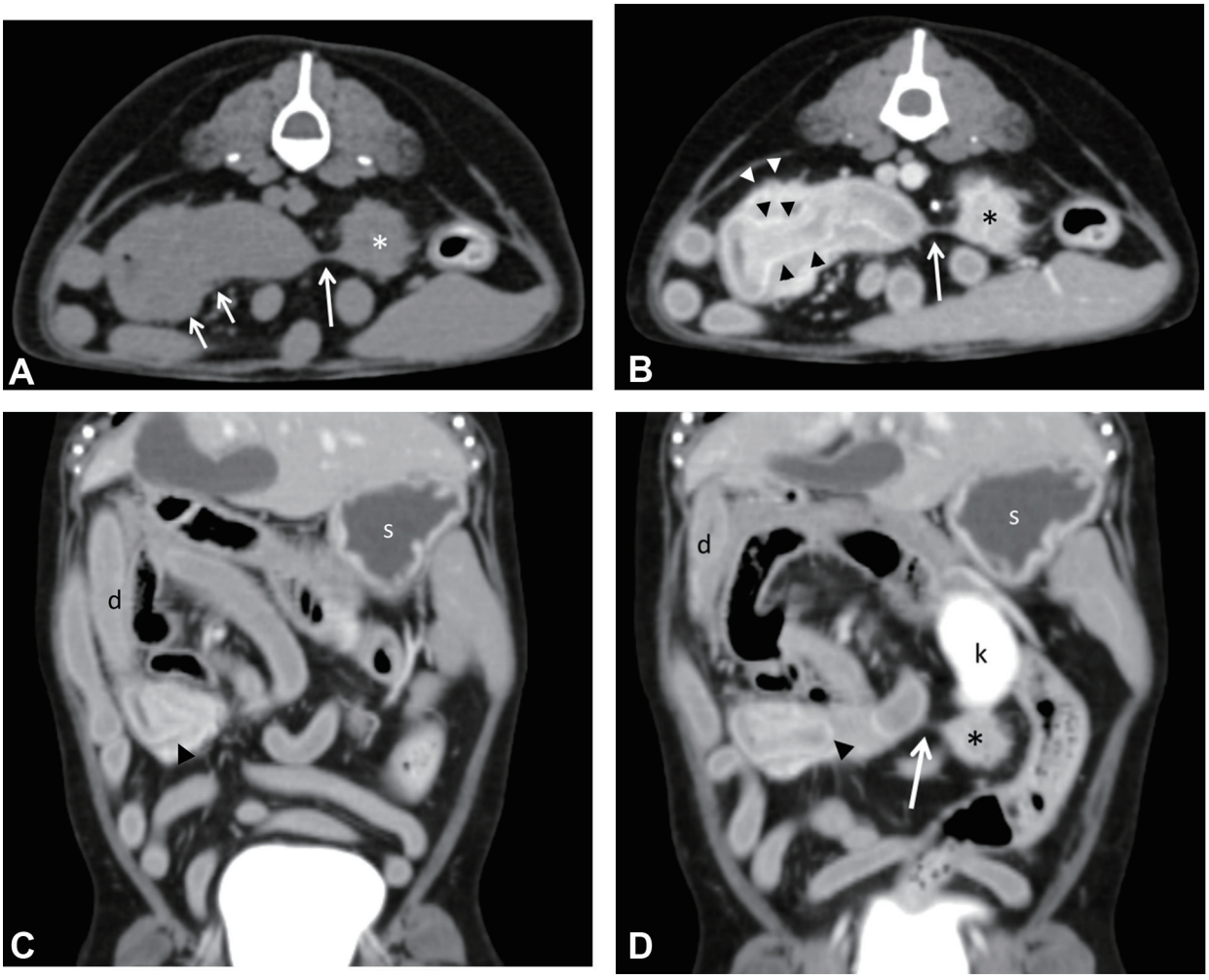


Fig. 2. Computed tomography of the left abdominal mass and duodenal mass. In the pre-contrast (A) CT image, the left abdominal mass (*) and duodenal mass (short arrows) showed homogeneous attenuation similar to the normal small intestine density. After contrast injection (B), the left abdominal mass (*) showed heterogeneous contrast enhancement, and the thickened duodenal wall exhibited contrast enhancement of the mucosal layer and muscular layer; the contrast enhancement was marked for the mucosal layer (black arrowheads). The heterogeneously enhanced region with an irregular margin at the dorsal duodenal wall surface (arrowheads) was the distal region of the normal right limb of the pancreas. A strand of soft tissue attenuating tissue connecting the left mass to the duodenal mass was found in pre- (A) and post-contrast (B and D) images. The strand was suspected to be peritoneal adhesion (long arrows). In the reformatted dorsal plane (C and D), the left abdominal mass (*) was located caudal to the left kidney (k), and the duodenal mass showed marked mucosal enhancement (black arrowhead). s=stomach, d=duodenum. The left side of the image is the right side of the dog.

gastrointestinal tract [16].

Regional granulomatous enteritis in dogs and Crohn's disease in humans have common histological features characterized by predominant neutrophilic inflammation with granuloma formation [6, 17]. In some patients with Crohn's disease, intestinal perforation or bowel obstruction due to granuloma formation has been reported [2, 7]. In this case, the histopathological findings were consistent with a previous report [17]; however, a granuloma arose from the descending duodenum, and there was no evidence of intestinal obstruction or fistula formation.

Although the etiology of the regional granulomatous enteritis is unclear, the pathogenesis of this condition is reported as the breakdown of immunological tolerance to luminal antigens [3, 6]. Non-idiopathic inflammation is more common in dogs, however, various etiologies including *Yersinia* and mycobacterial infections, foreign-body reactions and fungal disease can cause an intestinal granuloma [4, 5, 14, 15, 19]. Therefore, the underlying causes should be ruled out before diagnosis of idiopathic intestinal granuloma. In this dog, infectious organisms and foreign bodies were ruled out using Periodic acid-Schiff, Ziehl-Neelsen acid fast, Wright-Giemsa and Gram stains and diagnostic imaging.

The extent of wall thickening and integrity of wall layering are useful parameters in distinguishing inflammation from a tumor in ultrasonography [21]. The integrity of the

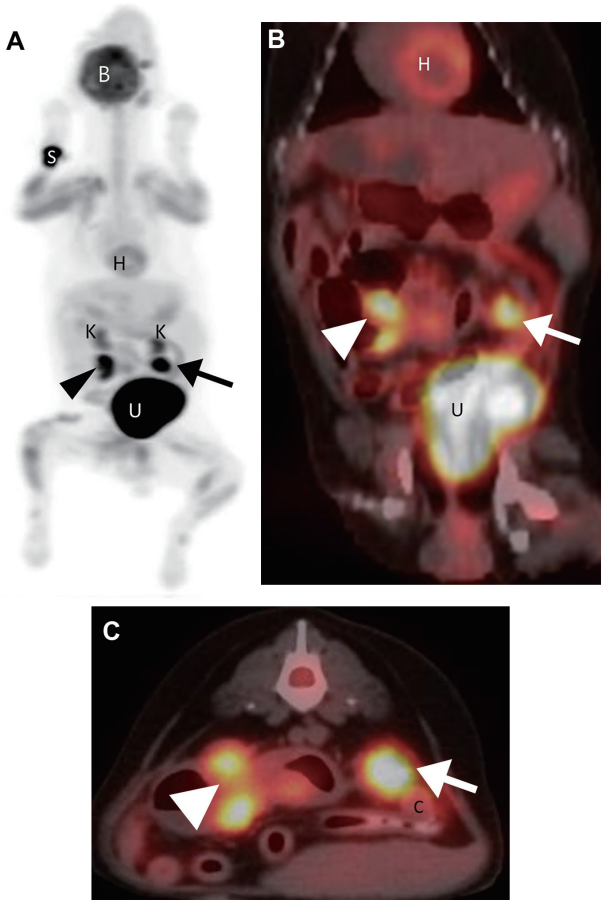


Fig. 3. Positron emission tomography and computed tomography images using FDG. (A) The maximum intensity projection view showed two focal FDG uptakes in the abdominal cavity and several physiologic uptakes (especially in the brain, heart, kidneys, and urinary bladder). (B-C) Fusion PET-CT images showing abnormal FDG uptakes. (B) In the dorsal plane, there were focal FDG uptakes in the duodenum (arrowhead) and in the left abdominal cavity (arrow). (C) The same findings were noted in the transverse plane. B=brain, H=heart, K=kidney, U=urinary bladder, S=injection site. The left side of the image is the right side of the dog.

intestinal wall layering is normal or reduced in enteritis, and most intestinal tumors lose the normal wall layering [21]. However, granulomatous enteritis can have an extensively thickened intestinal wall with loss of wall layering [5, 14]. In this dog, a thickened duodenum showing a mass-like appearance was found on ultrasonography, and therefore, we included only intestinal tumor and granulomatous enteritis into the differential lists.

The characteristic CT findings of Crohn's disease have been reported as mural contrastenhancement, intestinal wall thickening and stratification, obstruction due to wall thickening, enhanced fistulae and engorgement of the vasa recta correlated with active mucosal inflammation [7, 20]. In veterinary medicine, there has been no report of the CT

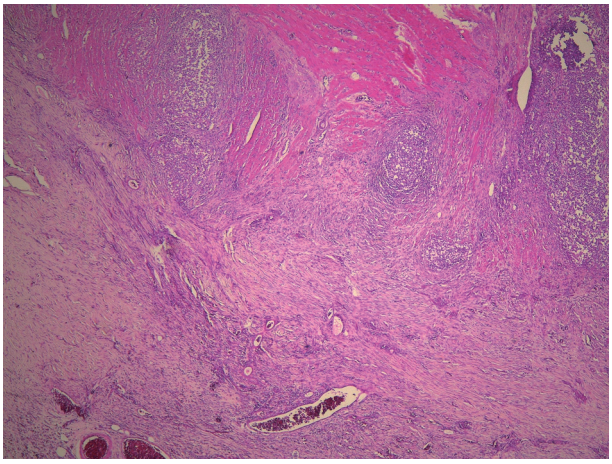


Fig. 4. Microscopic findings of the duodenal mass. The multiple pyogranulomas consist mainly of macrophages with some lymphocytes and neutrophils. Hematoxylin and eosin. 50 ×.

features of regional granulomatous enteritis. In this case, the CT examination demonstrated duodenal wall thickening with marked contrast enhancement; however, there were no obstructive lesions or fistulae. In addition, engorgement of the vasa recta was not seen on CT images.

PET-CT examination enables quantification and precise localization of FDG uptake in the body [12]. Inflammatory cells (e.g., macrophages, lymphocytes) like cancer cells could also express glucose transporters. In inflammatory conditions, both the number of inflammatory cells and expression of glucose transporters increase. These factors could contribute to increased FDG uptake [13]. Therefore, PET-CT findings should be correlated with other information including clinical history, other imaging findings and histologic examination, if the patient is suspected of both inflammation and neoplasm. In this case, the dog underwent a previous surgery, and a differential diagnosis of inflammation, such as granuloma, was needed for the left abdominal mass in light of increased FDG uptake. On the basis of the previous history of this dog, the left abdominal mass was suspected to be a suture granuloma. Suture granulomas, in humans, have been reported to lead to FDG accumulation within the lesion [9, 18, 23], and this case was consistent with these previous reports. Apart from the limitations in distinguishing inflammation from a neoplasm, PET-CT is a promising modality in the diagnosis of infection or inflammation [13]. In particular, PET-CT is helpful in assessing the extent and severity of inflammatory lesions and in evaluating the result after treatment in Crohn's disease [12]. In the present case, however, the dog did not undergo a follow-up PET-CT examination due to recovery without clinical signs.

The treatment of idiopathic IBD usually involves a combination of dietary control, antibiotics and immunosuppressive agents, regardless of the histological type [6]. In Crohn's disease in humans, surgical resection is usually indicated for patients who fail to respond to drug or dietary therapy [22]. In a dog with regional enteritis, surgical resection of

the affected portion of the bowel loops palliated the clinical signs [1]. This dog did not undergo long-term follow-up, but it recovered completely after surgical resection of the duodenal granuloma.

In the present case, it was not possible to distinguish granulomatous enteritis from intestinal tumor by diagnostic imaging in spite of the multiple modalities. Few cases of regional granulomatous enteritis have been reported in the veterinary literature, and the human literature indicates that regional granulomatous enteritis may have similar imaging features to those of intestinal tumors. Ultrasonography, CT and PET-CT were helpful in determining the shape, location and extension of the duodenal mass and in excluding metastasis.

ACKNOWLEDGMENTS. This study was supported in part by the Basic Science Research Program through the National Research Foundation of Korea (NRF) funded by the Ministry of Education, Science and Technology (2012R1A1A1040407) and by the Animal Medical Institute of Chonnam National University. We thank Jung-Jin Roh and Chan-Yong Kim for technical assistance in PET-CT imaging.

REFERENCES

1. Bright, R., Jenkins, C., DeNovo, R., McCrackin, M. and Toal, R. 1994. Chronic diarrhoea in a dog with regional granulomatous enteritis. *J. Small Anim. Pract.* **35**: 423–426. [CrossRef]
2. Bruining, D. H., Siddiki, H. A., Fletcher, J. G., Tremaine, W. J., Sandborn, W. J. and Loftus, E. V. Jr. 2008. Prevalence of penetrating disease and extraintestinal manifestations of Crohn's disease detected with CT enterography. *Inflamm. Bowel Dis.* **14**: 1701–1706. [Medline] [CrossRef]
3. Elson, C. 1999. Experimental models of intestinal inflammation: new insights into mechanisms of mucosal homeostasis. p. 1024. *In*: Mucosal Immunology (Orgro, P. l., Lamm, M. E., Bienestock, J., Mestecky, J., Strober, W. and McGhee, J. R. eds.), Academic Press, San Diego.
4. German, A. J., Hall, E. J. and Day, M. J. 2003. Chronic intestinal inflammation and intestinal disease in dogs. *J. Vet. Intern. Med.* **17**: 8–20. [Medline] [CrossRef]
5. Graham, J. P., Newell, S. M., Roberts, G. D. and Lester, N. V. 2000. Ultrasonographic features of canine gastrointestinal pythiosis. *Vet. Radiol. Ultrasound* **41**: 273–277. [Medline] [CrossRef]
6. Hall, E. J. and German, A. J. 2008. Inflammatory Bowel Disease. pp. 312–329. *In*: Small Animal Gastroenterology (Steiner, J. M. ed.), Schlütersche, Hannover.
7. Huprich, J. E. and Fletcher, J. G. 2009. CT enterography: principles, technique and utility in Crohn's disease. *Eur. J. Radiol.* **69**: 393–397. [Medline] [CrossRef]
8. Jergens, A. E. 2002. Understanding gastrointestinal inflammation—implications for therapy. *J. Feline Med. Surg.* **4**: 179–182. [Medline] [CrossRef]
9. Kikuchi, M., Nakamoto, Y., Shinohara, S., Fujiwara, K., Tona, Y., Yamazaki, H., Kanazawa, Y., Kurihara, R., Imai, Y. and Naito, Y. 2012. Suture granuloma showing false-positive finding on PET/CT after head and neck cancer surgery. *Auris Nasus Larynx* **39**: 94–97. [Medline] [CrossRef]
10. Lewis, D. C. 1995. Successful treatment of regional enteritis in a dog. *J. Am. Anim. Hosp. Assoc.* **31**: 170–173. [Medline]
11. Loftus, E. V. Jr. 2004. Clinical epidemiology of inflammatory bowel disease: incidence, prevalence, and environmental influences. *Gastroenterology* **126**: 1504–1517. [Medline] [CrossRef]
12. Louis, E., Ancion, G., Colard, A., Spote, V., Belaiche, J. and Hustinx, R. 2007. Noninvasive assessment of Crohn's disease intestinal lesions with (18)F-FDG PET/CT. *J. Nucl. Med.* **48**: 1053–1059. [Medline] [CrossRef]
13. Love, C., Tomas, M. B., Tronco, G. G. and Palestro, C. J. 2005. FDG PET of infection and inflammation. *Radiographics* **25**: 1357–1368. [Medline] [CrossRef]
14. Malik, R., Hunt, G. B., Bellenger, C. R., Allan, G. S., Martin, P., Canfield, P. J. and Love, D. N. 1999. Intra-abdominal cryptococcosis in two dogs. *J. Small Anim. Pract.* **40**: 387–391. [Medline] [CrossRef]
15. Martins, T. B., Kommers, G. D., Trost, M. E., Inkelmann, M. A., Fighera, R. A. and Schild, A. L. 2012. A comparative study of the histopathology and immunohistochemistry of pythiosis in horses, dogs and cattle. *J. Comp. Pathol.* **146**: 122–131. [Medline] [CrossRef]
16. Mekhjian, H. S., Switz, D. M., Melnyk, C. S., Rankin, G. B. and Brooks, R. K. 1979. Clinical features and natural history of Crohn's disease. *Gastroenterology* **77**: 898–906. [Medline]
17. Morson, B. C. 1971. Histopathology of Crohn's disease. *Scand. J. Gastroenterol.* **6**: 573–575. [Medline] [CrossRef]
18. Nagar, H. 1993. Stitch granulomas following inguinal herniotomy: a 10-year review. *J. Pediatr. Surg.* **28**: 1505–1507. [Medline] [CrossRef]
19. Papazoglou, L. G., Tontis, D., Loukopoulos, P., Patsikas, M. N., Hermanns, W., Kouti, V., Timotheou, T., Liapis, I., Tziris, N. and Rallis, T. S. 2010. Foreign body-associated intestinal pyogranuloma resulting in intestinal obstruction in four dogs. *Vet. Rec.* **166**: 494–497. [Medline] [CrossRef]
20. Paulsen, S. R., Huprich, J. E., Fletcher, J. G., Booya, F., Young, B. M., Fidler, J. L., Johnson, C. D., Barlow, J. M. and Earnest, F. T. 2006. CT enterography as a diagnostic tool in evaluating small bowel disorders: review of clinical experience with over 700 cases. *Radiographics* **26**: 641–657, discussion 657–662. [Medline] [CrossRef]
21. Penninck, D., Smyers, B., Webster, C. R., Rand, W. and Moore, A. S. 2003. Diagnostic value of ultrasonography in differentiating enteritis from intestinal neoplasia in dogs. *Vet. Radiol. Ultrasound* **44**: 570–575. [Medline] [CrossRef]
22. Rampton, D. S. 1999. Management of Crohn's disease. *BMJ* **319**: 1480–1485. [Medline] [CrossRef]
23. Takahara, K., Kakinoki, H., Ikoma, S., Udo, K., Tobu, S., Satoh, Y., Tokuda, Y., Noguchi, M., Aoki, S. and Uozumi, J. 2013. Suture Granuloma Showing False-Positive Findings on FDG-PET. *Case Rep.Urol.* **2013**: 472642. [Medline]